Article published online: 2021-10-04

Pictorial essay: Salivary gland imaging

Rajul Rastogi, Sumeet Bhargava[1], Govindarajan Janardan Mallarajapatna[2], Sudhir Kumar Singh[3]

Yash Diagnostic Center, Yash Hospital and Research Center, Moradabad, [1]Department of Radiology and Imaging, Subharti Medical College, Meerut, [3]Department of ENT, Kothiwal Dental College and Research Center, Moradabad, Uttar Pradesh, [2]Department of Imaging and Interventions, Health Care Global Bangalore Institute of Oncology, Bangalore, Karnataka, India

Correspondence: Dr. Rajul Rastogi, Yash Hospital and Research Center, Moradabad, Uttar Pradesh - 244001, India.
E-mail: eesharastogi@gmail.com

Abstract

Salivary glands are the first organs of digestion secreting their digestive juices into the oral cavity. Parotid, submandibular, and sublingual glands are the major paired salivary glands in the decreasing order of their size. In addition, multiple small minor salivary glands are noted randomly distributed in the upper aerodigestive tract, including paranasal sinuses and parapharyngeal spaces. The imaging is directed to the major salivary glands. Commonly used imaging methods include plain radiography and conventional sialography. Recently, high-resolution ultrasonography (HRUS) is being increasingly used for targeted salivary gland imaging. However, the advent of cross-sectional imaging techniques such as computed tomography (CT) and magnetic resonance imaging (MRI) have revolutionized the imaging of salivary glands. This article illustrates the role of imaging in evaluating the variegated disease pattern of the major salivary glands.

Key words: Computed tomography; imaging; magnetic resonance imaging; salivary glands

Introduction

Parotid, submandibular, and sublingual glands are the major paired salivary glands of the body acting on the first step of the digestion process.

The parotid gland is the largest salivary gland and is composed of adipose and glandular tissues in nearly equal proportions, making it appear nearly isodense/isointense to fat on computed tomography/magnetic resonance imaging (CT/MR) images. The parotid gland is divided into the larger superficial and smaller deep lobes by the retromandibular or facial vein. It is located posterior to the ramus of mandible and drains via the Stenson's duct traversing superficial to the masseter muscle and passing through the buccinator muscle before finally opening into the oral cavity at the ipsilateral 2nd maxillary molar. The distal part of facial nerve and its terminal branches passes through the parotid parenchyma. Multiple nodes are located superficially and within the parotid gland. Accessory parotid gland is noted in 20% subjects and is usually located anterior to the main parotid and superior to the Stenson's duct draining in to the latter through an accessory duct.

The submandibular gland is the second largest salivary gland and is located in the floor of the mouth adjacent to the posterior body of mandible along the free edge of the mylohyoid muscle. The amount of adipose tissue is relatively lower than that of parotid gland. The lingual nerve and submandibular ganglion are noted superficial to the submandibular gland while the hypoglossal nerve lies deep to it. It drains through the Wharton's duct in the anterior sublingual region at the papilla in paramidline location.

Sublingual gland is the smallest major salivary gland. It lies submucosally adjacent to the anterior mandible in parasymphyseal location. The Wharton's duct and lingual nerve separate the sublingual gland from the medial genioglossus muscle. It opens via multiple ducts usually 20 in number (known as ducts of Rivinus) directly into the floor of mouth along sublingual papillae and folds. Occasionally, some of the ducts unite to form the Bartholin's duct that drain into the Wharton's duct.

The common clinical indications of salivary gland imaging are pain and swelling. Imaging is useful in identifying the

Access this article online

Quick Response Code:

Website: www.ijri.org

DOI: 10.4103/0971-3026.111487

masses of salivary glands and also in differentiating them from the masses/pathologies of adjacent cervical spaces, especially parapharyngeal, masticator, and submental spaces and mandibular lesions. Nodal masses, peripheral nerve schwannomas, and masseteric hypertrophy may mimic tumors of salivary glands clinically. In proven cases of salivary gland tumors, imaging helps in delineating the extent of the lesion and invasion of adjacent cervical spaces, skull base, mandible, and nerves/meninges. The disease of major salivary gland can be broadly categorized into the inflammatory, neoplastic, systemic, and congenital conditions.

Imaging Armamentarium for Salivary Gland Imaging Includes:[1–3]

- Plain radiography
- Sialography (conventional, CT, MRI)
- High-resolution ultrasonography (HRUS)
- Computed tomography (CT)
- Magnetic resonance imaging (MRI)
- Radionuclide scintigraphy

Plain Radiography

This is the simplest, oldest, and cheapest way of studying the salivary glands. It is useful in detecting ductal calculi, calcifications (as in hemangioma and lymph nodes), and adjacent osseous lesions. Only one-fifth of the salivary ductal calculi are radiolucent.

Parotid gland radiography requires posteroanterior projection with extended chin, open mouth, and cheeks blown out to delineate Stenson's duct lesion. Submandibular gland radiography requires posteroanterior and ipsilateral oblique projection with extended chin, open mouth, and tongue depressed by patients' finger [Figure 1].

Sialography

It refers to the evaluation of the ductal system of the salivary glands. It is considered the gold standard technique for studying the ductal morphology. It is commonly used for parotid and submandibular glands and its main indication is chronic sialadenitis unrelated to sialolithiasis [Figure 2].

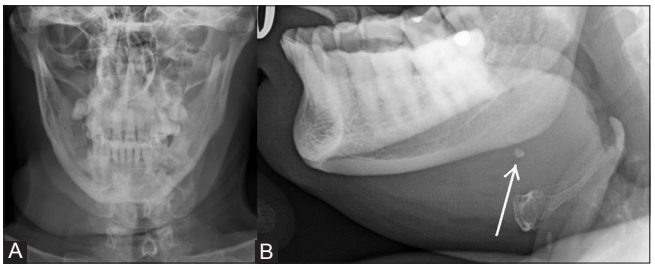

Figure 1 (A, B): Plain radiograph of the submandibular region in AP (A) and lateral oblique (B) projection showing soft tissue swelling associated with a small calculus (arrow) visible on lateral oblique view taken with depressed tongue

Acute sialadenitis is a contraindication for sialography. Irregular pooling of contrast and ductal obstruction without presence of calculus are indirect signs of malignancy.

Sialography is rarely used for sublingual imaging because of numerous small ducts opening directly into the floor of mouth. Sublingual glands may however be visualized in an anatomic variation where the Bartholin's duct is outlined following injection of the contrast medium into the Wharton's duct.

It is usually performed through digital subtraction method following retrograde intracannular injection of the water-soluble, iodinated, contrast medium into the Stenson's/Wharton's duct opening to opacify the ductal system. However, 3DCT performed especially with cone-beam CT following injection of the contrast medium into the ductal system without intravenous injection of contrast can provide images similar to or better than conventional sialography and is often referred to as CT sialography.[4] MR Sialography, by contrast, delineates the ductal system of the gland without injection of ductal/intravenous contrast by utilizing the highly

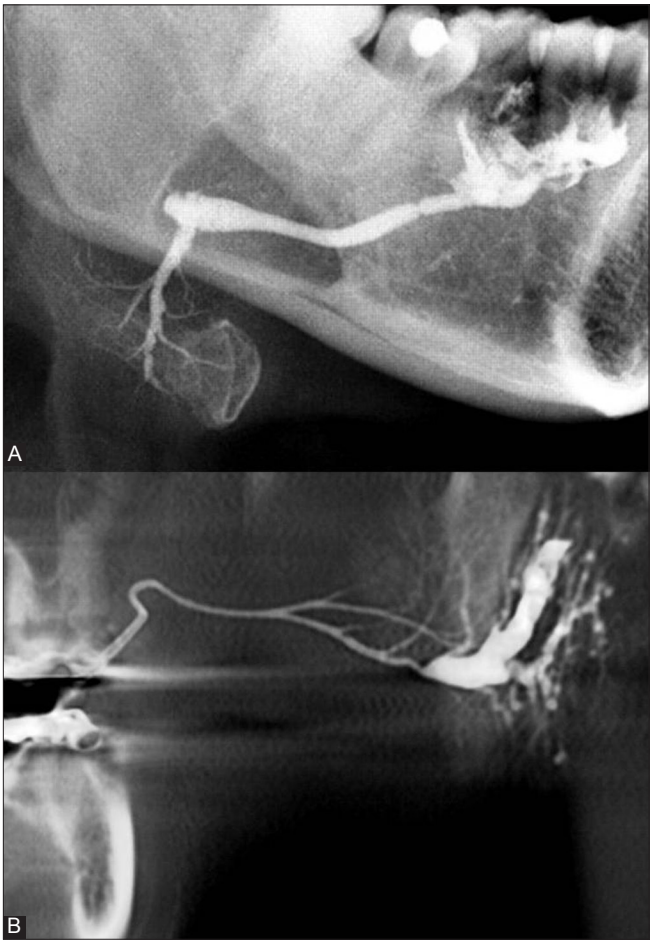

Figure 2 (A, B): Conventional sialography of submandibular (A) and parotid glands (B) showing ductal system

fluid-sensitive sequences similar to that used for magnetic resonance cholangiopancreatography (MRCP) [Figure 3]. MR Sialography can be performed in patients of acute sialadenitis. Prior administration of a sialogogue agent may improve ductal visualization in MR Sialography.[5] MR Sialography has poor spatial resolution as compared to conventional sialography.[6]

High-resolution Ultrasonography

It is a quick and noninvasive method of evaluating parotid and submandibular glands. Both glands appear homogeneously hyperechoic on HRUS, and retromandibular vein can be noted within the parotid gland [Figure 4]. It is performed by a high-frequency linear (7-10 MHz) transducer. It helps in differentiating cystic from solid lesions and also aids in guiding the exact site of Fine **N**eedle **A**spiration **C**ytology (FNAC) in suspected salivary gland lesions.[7]

When combined with color Doppler imaging, it helps in assessing the vascularity and nature of the lesion (malignant lesions of salivary glands are highly vascular as compared to their benign counterparts – peripheral vascularity with hypovascular central area in the tumoral lesion is highly suggestive of pleomorphic adenoma). RI and PI values of greater than 0.7 and 1.2, respectively, coupled with high PSV (greater than 44.3 cm/s), ill-defined margins, and nodal involvement with central vascularity are highly indicative of malignant salivary gland lesion.[8,9]

In experienced hands, it helps in differentiating intra-parotid nodes from true intraparenchymal lesions, picking soft calcifications/diffuse lesions and detecting major ductal dilatation with intraductal calculi [Figure 5]. However, it cannot optimally evaluate the deep lobe of the parotid gland.

CT and MRI

These cross-sectional studies help in true and near complete imaging of the salivary glands [Figures 6-8]. MRI, because of its multiplanar capability and higher soft tissue resolution, has an upper hand over CT in demonstrating the extent of lesion and their perineural/meningeal spread. However, CT (especially cone-beam CT) demonstrates the osseous lesions/extension and calcification/calculus better than MRI. Noncontrast CT may be enough in cases of sialolithiasis. However, ductal system is not optimally evaluated by any of these techniques.

These studies are often performed after intravenous injection of the contrast media for better delineation of the anatomy and the extent of lesion. Diffusion-weighted (DW) images and gadolinium-enhanced dynamic MR (Gd-MRI) imaging have proven to be very useful in differentiating benign from malignant tumors.[10,11] DW images can be used to calculate apparent diffusion coefficient (ADC) values, which are different for different salivary gland tumors. Gd-MR with dynamic imaging using 120 s as cut-off for time to peak enhancement and 30 % wash-out ratio can differentiate benign and malignant tumors as the latter take less time for peak enhancement and show rapid wash-out. Plateau type of time–intensity curve in dynamic Gd-MR coupled with low ADC values is also highly suggestive of malignancy. Proton MR Spectroscopy

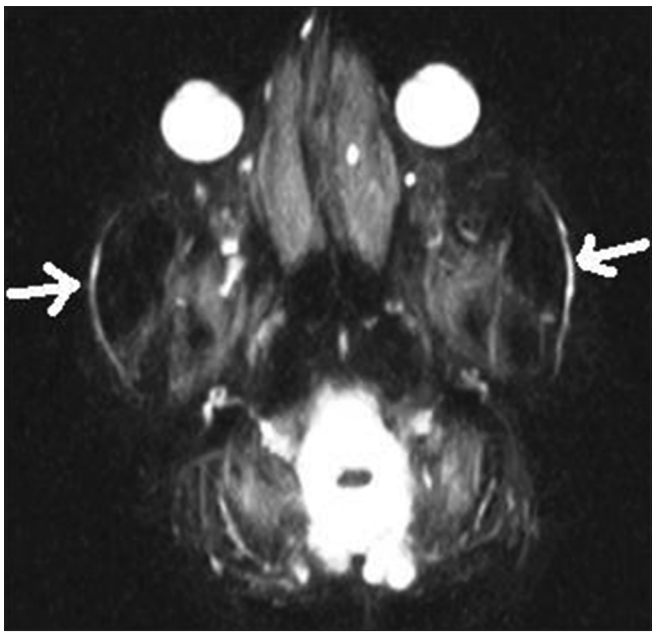

Figure 3: MR sialography shows bilateral Stemson's duct (arrows)

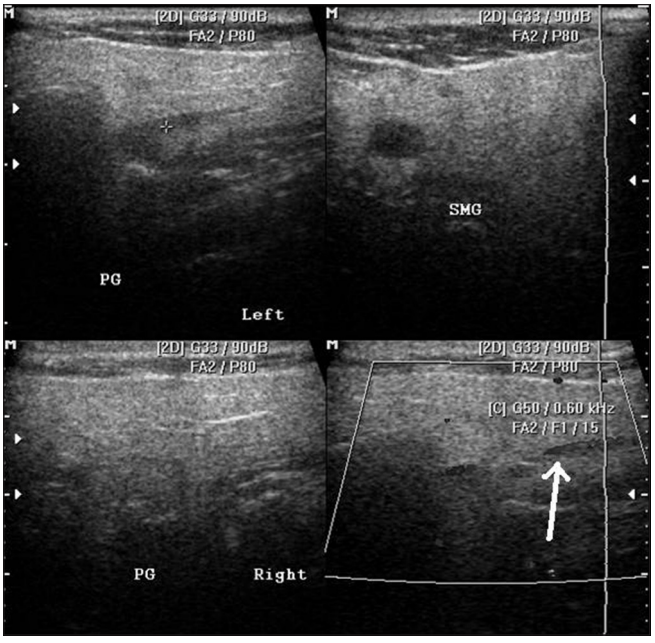

Figure 4: HRUS images showing normal parotid and submandibular glands (top row) and retromandibular vein in the parotid gland (arrow)

has also been described for differentiation of benign from malignant tumors by some authors. Choline/creatinine ratios are significantly lower in malignant than in benign salivary gland tumors.[12]

Radionuclide Imaging

It is a rarely used technique for salivary gland imaging. Sodium pertechnetate (Tc^{99}) is actively concentrated and secreted by salivary gland cells while it is not taken up by majority of neoplastic lesions, hence the latter appear as *cold spots*. Warthin's tumor is an exception to the rule and appears as a *hot spot*.

Actively dividing cells take up Gallium-67; hence it is useful in detecting diffuse inflammatory/neoplastic processes such as sarcoidosis and lymphoma.

Positron emission tomography (PET) imaging using 2-deoxy-2-[18F] fluoro-d -glucose (FDG) can be used to differentiate benign from malignant tumors of the salivary glands as the former appear as *cold spots* with the exception of Warthin's tumor and oncocytoma.[13]

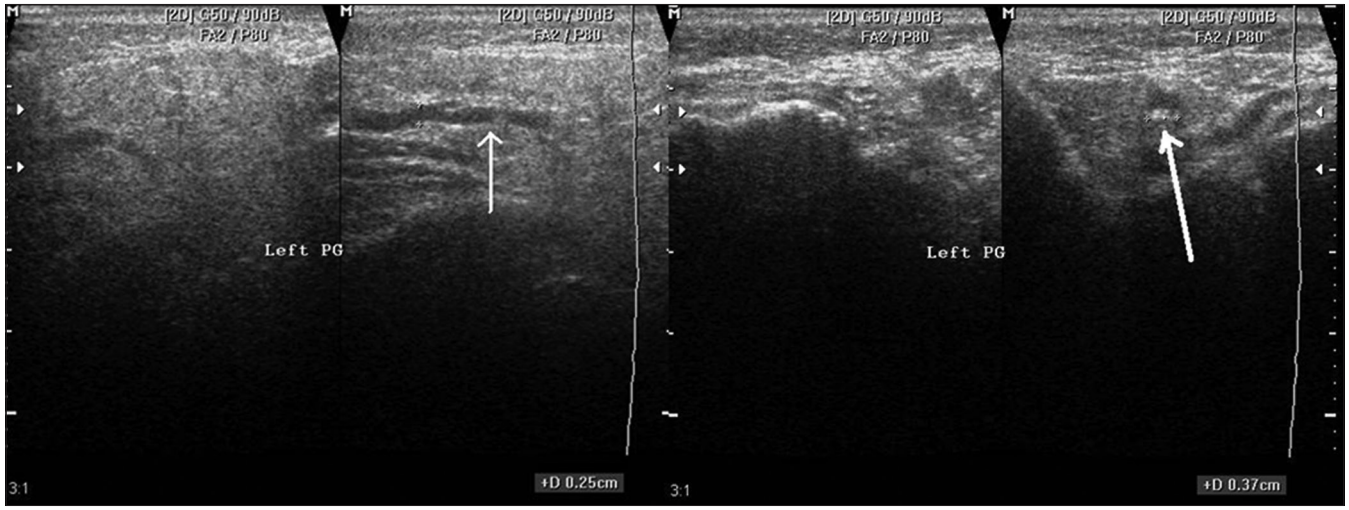

Figure 5: HRUS images show altered echopattern of the parotid gland with ductal dilatation (thin arrow) and small calculus (thick arrow) at its terminal end

Figure 6: Non-contrast axial CT image showing submandibular sialolithiasis on right side (white arrow) and normal gland on left side

Figure 7: Non-contrast axial CT image show normal appearing parotid (white arrows) gland in a young subject

Inflammatory Diseases of Salivary Glands

Sialolithiasis is the second commonest cause of sialadenitis next only to mumps and probably the commonest cause of unilateral enlargement of the salivary glands. Sialolithiasis is commonest in the submandibular gland and may cause diffuse or focal enlargement of the gland. Imaging is useful in detecting and defining the location of nonpalpable/multiple calculi. Rarely, a mucus plug instead of the calculus may be a cause of ductal obstruction and consequent acute sialadenitis, often referred to as *Kussmaul disease.*

Conventional sialography, HRUS, and CT can detect sialolithiasis with a high degree of sensitivity.[14] HRUS is however inferior to CT in differentiating a solitary large ductal calculus from a cluster of small calculi. MRI sialography is useful in cases of chronic sialadenitis when sialolithiasis has been ruled out by the aforementioned studies, especially to look for strictures following passage of calculus. Autoimmune sialadenitis reveals pruning/truncation of major ducts and globular peripheral collections on MR sialography as periphery of the gland is the usual site of initiation of this pathologic process. Presence of microabscesses may mimic peripheral collections of the autoimmune process.

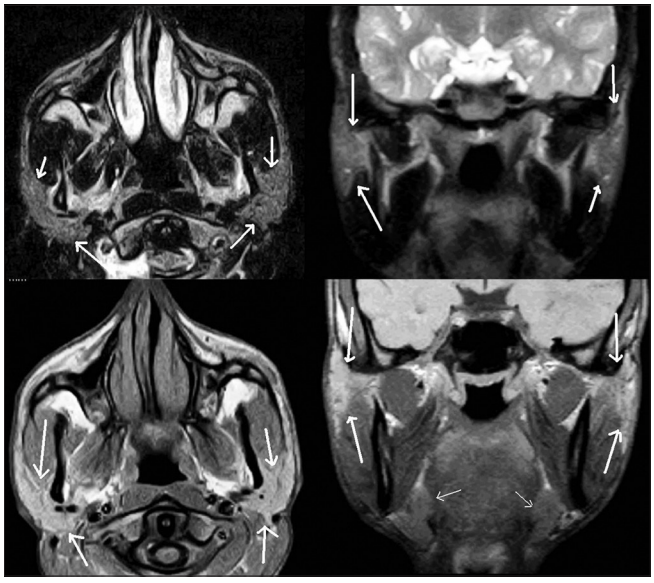

Figure 8: Non-contrast T2W axial & coronal images (top row) and T1W axial and coronal images showing parotid (thick white arrows) and submandibular glands (thin white arrow)

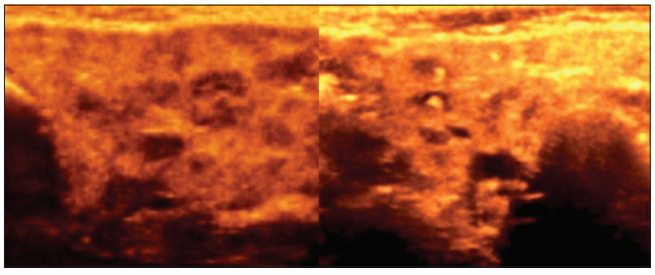

Figure 10: 3D HRUS image shows parotid gland with altered echopattern and small calculi in a case of sialadenitis

HRUS shows diffusely enlarged and tender gland with diffuse decrease in echogenicity, heteroechoic pattern (due to small focal lesions) and with diffuse increase in vascularity with or without abscess formation in acute stages [Figures 9-11]. In chronic stages, the gland may be normal or small in size with reduced echogenicity and vascularity and heteroechoic pattern.

Sialadenitis manifests as moderate to intensely enhancing, diffusely enlarged salivary gland with or without abscess formation, and intraparenchymal/regional lymphadenopathy on CT/MR imaging [Figures 12-14]. There is associated soft tissue stranding/thickening of adjacent fat and cervical fascia. As MRI is more sensitive to edema, it picks up early sialadenitis and even inflammation of ductal walls (sialodochitis). MRI in coronal plane is very helpful in delineating the relationship of salivary gland lesions with other structures in the floor of mouth as in ranula (a mucous retention cyst) and in demonstrating the invasion of skull base especially in parotid lesions.

Ranula refers to a mucus retention pseudocyst occurring in the floor of the mouth within the sublingual space commonly

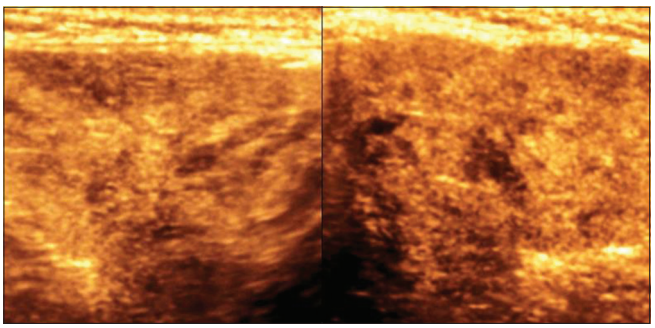

Figure 9: 3D HRUS image shows enlarged submandibular gland with altered echopattern in a case of sialadenitis

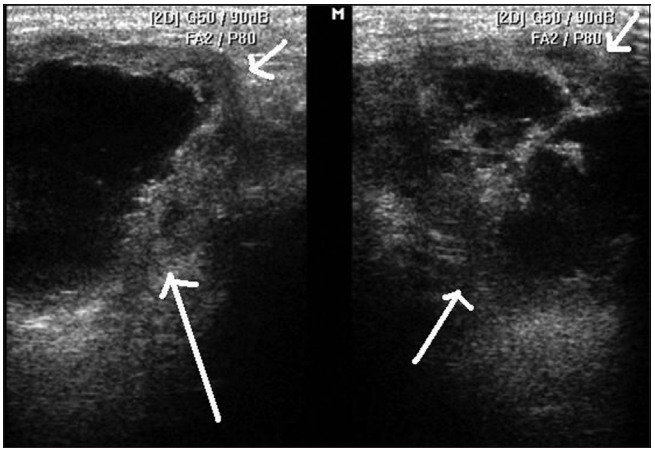

Figure 11: HRUS image shows submandibular gland abscess (white arrows)

Figure 12: Contrast-enhanced axial CT image shows hypodense, enlarged right submandibular gland with calculus (thick white arrow) and thickening of adjacent fascia (thin white arrow)

from the sublingual gland following traumatic extravasation of the salivary secretions or following obstruction of the draining duct. Ranula is said to be plunging when it extends anteriorly into the submental space or posteriorly into the submandibular space through either the dehiscence or the posterior free margin of the mylohyoid muscle. It appears as a smooth-walled and fluid-dense/fluid-intense lesion devoid of internal septations on CT/MR images. Presence of anterior tapering into the sublingual space (tail sign) is typical of ranula when it plunges posteriorly. Presence of enhancing walls is indicative of superadded infection.

The important differential diagnosis of abscess within the salivary glands is superinfected cysts in HIV patients, suppurative nodes in the parotid gland, and cystic degeneration/superinfection of the existing neoplasm.

Chronic sialadenitis usually manifests as reduction in parenchymal volume of gland associated with multifocal intraglandular calcifications and rarely a solitary large ductal calculus.

Neoplastic Diseases of Salivary Glands

Salivary gland neoplasms usually present as painless, solitary masses. The risk of malignancy is usually higher in the smaller salivary glands. Majority of the benign lesions are pleomorphic adenoma with Warthin's tumor,

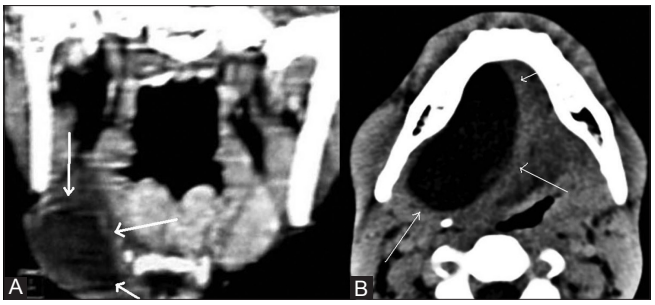

Figure 13 (A, B): Contrast-enhanced coronal CT image (A) shows submandibular mucocele on right side (thick white arrow) while axial CT image (B) shows right sublingual gland mucocele (thin white arrows)

monomorphic adenoma, oncocytoma, myoepithelioma, lipoma, and hemangioma accounting for the other small number of benign lesions. Pleomorphic adenoma is more common in middle-aged females. Oncocytoma and Warthin's tumor are predominantly noted in parotid gland. Multifocal masses within the parotid gland are either enlarged lymph nodes or Warthin's tumor.

Malignant lesions include mucoepidermoid carcinoma, adenoid cystic carcinoma, undifferentiated carcinoma, adenocarcinoma, and squamous carcinoma. Most common malignant lesion occurring in parotid gland is mucoepidermoid carcinoma while in submandibular gland, adenoid cystic carcinoma is the commonest associated with high propensity for perineural extension.

Malignant lymphadenopathy within the parotid may be secondary to cutaneous malignancies, especially basal cell carcinoma, squamous cell carcinoma, and melanoma; lymphoma and rarely secondary to malignancies involving upper aerodigestive tract.

CT and MRI are the usual investigations used for evaluating known/suspected salivary gland masses [Figures 15-17]. Imaging cannot distinguish between different histologic types as all tumors are isoattenuating to glandular parenchyma on CT and hypointense to gland on T1W MR image and all of them enhance on postcontrast CT and MR images. However, both the modalities can sensitively differentiate between solid and cystic lesions.

MRI examination is preferred over CT when associated neural (facial, trigeminal, hypoglossal, and lingual nerves) and meningeal involvement is suspected. The signs of malignancy on imaging include invasion of adjacent structures (nerves, bone, skull base, meninges, and adjacent cervical spaces) and rupture of capsule in pleomorphic adenoma, all of which are better delineated by MRI. Postgadolinium, fat-suppressed T1W images are preferred for determining the invasion. Ill-defined margins of the tumor on postcontrast images are also highly suggestive of malignancy.[15]

Figure 14: Contrast-enhanced axial MR image shows severe parotitis on left side (white arrows)

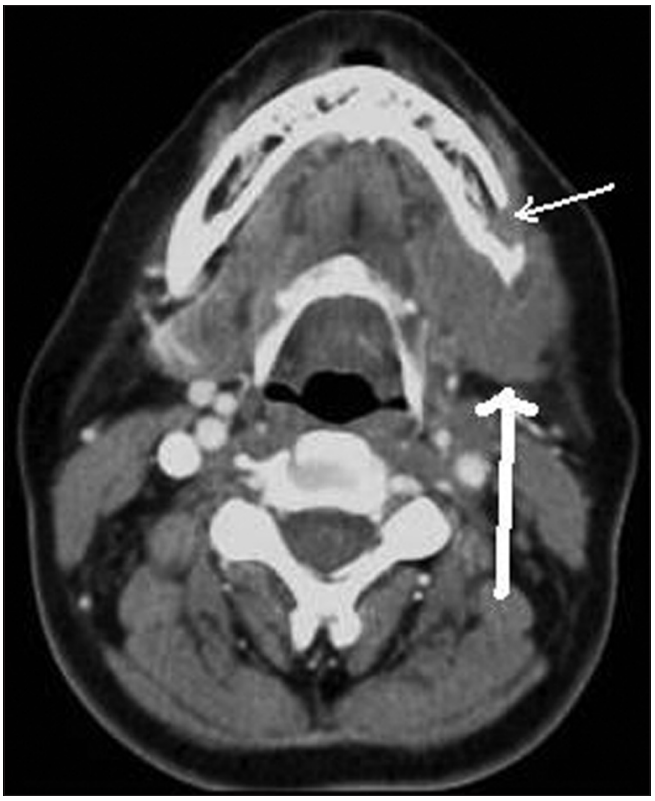

Figure 15: Contrast-enhanced axial CT image shows enlarged left submandibular gland (thick white arrow) associated with destruction of the adjacent mandible (thin white arrow) in a case of adenoid cystic carcinoma

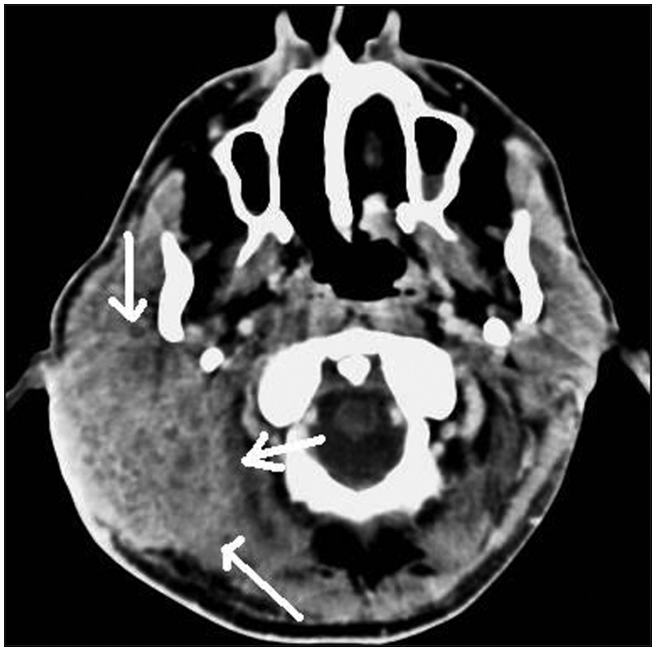

Figure 16: Contrast-enhanced axial CT image shows malignant pleomorphic adenoma of right parotid gland (white arrows

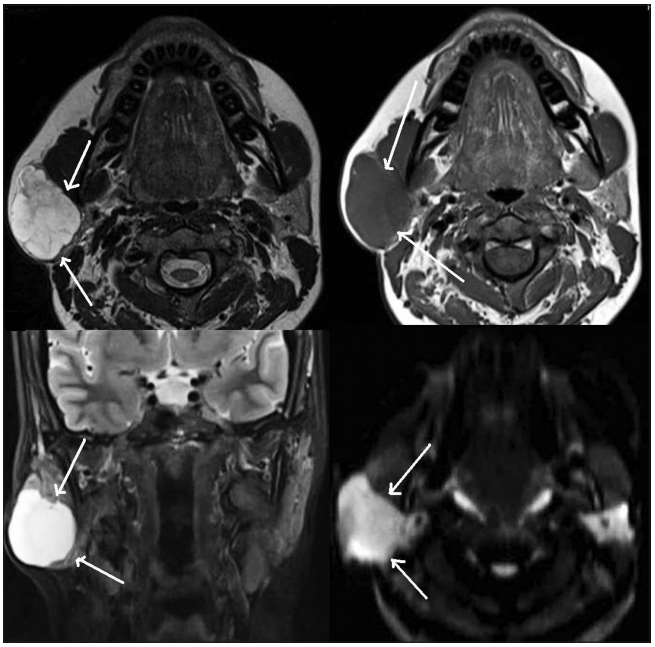

Figure 17: Non-contrast T2 & T1W axial images (upper row) and T2W coronal & DW axial images (lower row) show pleomorphic adenoma of right parotid gland (white arrows)

Pleomorphic adenoma is usually homogeneously hyperintense on T2W, while presence of mass with low-to-intermediate intensity on T2W images is more indicative of a malignant lesion. Warthin's tumor is an exception appearing hypointense on T2W images. Oncocytoma is isointense to the glandular parenchyma on fat-suppressed T2W and postcontrast T1W images.[16]

Radionuclide scintigraphy is preferred in suspected Warthin's tumor and oncocytoma as they appear as hot spots in contrast to all the other benign and malignant lesions. Multiple salivary gland lesions are an indication of scintigraphy to detect Warthin's tumor among the multiple lesions as they can be followed conservatively.

Salivary Gland Involvement in Systemic Disease

Major systemic diseases involving salivary glands are autoimmune processes predominantly including Sjögren's syndrome (including Mikulicz disease) and sarcoidosis. Salivary gland involvement can also occur in HIV disease and following radiation exposure. Imaging reveals diffuse enlargement of the gland in early stages with/without the presence of focal masses, nodules, cysts, nodes, calculi, or calcifications and features of chronic sialadenitis in later stages. Sarcoidosis and Sjögren's syndrome are associated with high incidence of calculi while the latter has a high propensity for lymphoma of parotid. Recently, MR microscopy has been tried to study and stage the parotid gland involvement in patients with Sjögren's syndrome.

MR microscopy refers to the imaging of the parotid gland with small surface coil less than 100 mm in diameter to obtain images of higher spatial resolution (47 mm in a study by Takagia, *et al*.) than that obtained by usual coils.[17] This allows better evaluation (quantitative rather than qualitative assessment) of parotid gland in patients of Sjögren's disease to determine the severity of disease.[17] The parameters usually involved are the quantification of glandular fat, intact glandular lobules, and number of sialectatic foci.

Bilateral, diffuse, and painless enlargement of the salivary gland referred to as *sialosis* occurs in diabetes mellitus, chronic alcoholism, hypothyroidism, malnutrition, and rarely secondary to certain drugs (antibiotic, antipsychotics. and diuretics).[18] HRUS reveals a hyperechoic gland without increased vascularity or focal lesions.

Multiple granulomatous diseases including Wegener's disease, tuberculosis, syphilis, and fungal infections may involve salivary glands either diffusely or focally [Figures 18 and 19].

Kimura disease (combination of eosinophilia and lymphoid proliferation of cervical nodes and salivary glands), actinomycosis, amyloidosis, and hematogenous metastases (usually thyroid and renal in origin) are very rare causes of salivary gland involvement especially the parotids.

CT reveals hyperattenuating glandular parenchyma in both acute and chronic stages associated with enlargement in acute and loss of glandular volume in chronic stages. However, on MRI images, the gland is hyperintense on T2W images in acute and relatively hypointense in chronic stages.

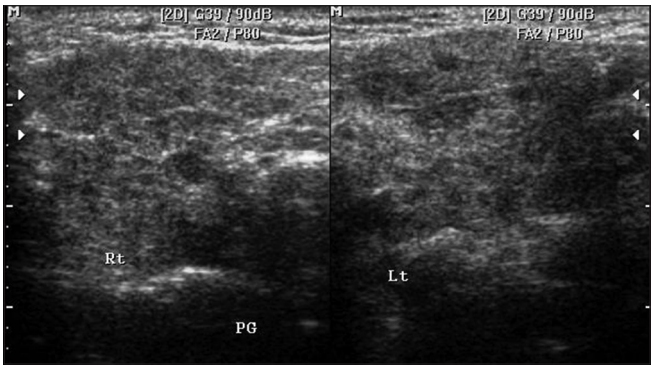

Figure 18: HRUS images show bilateral diffusely hypoechoic parotid gland with small hypoechoic nodular lesions in a patient of granulomatous parotitis

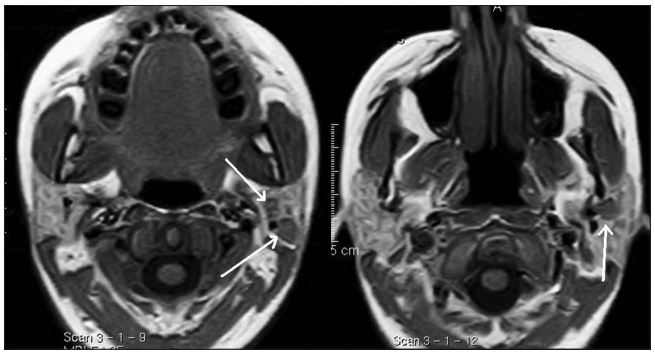

Figure 19: Non-contrast T1W axial images show intraparotid adenopathy (white arrows) with altered appearance in a case of tuberculosis of left parotid gland

Figure 20: T2W sagittal MR image shows a sublingual epidermoid cyst (white arrows)

Congenital Lesions of the Salivary Glands

These include cysts (type I branchial cyst, salivary cysts, dermoid, and epidermoid cysts), lipoma, hemangioma, lymphangioma, sialolipoma, and sarcoma [Figure 20].[19] Majority occur in the parotid glands and some of them such as lipoma, hemangioma, dermoid cyst, and lymphangioma reveal characteristic features on CT and MR imaging as elsewhere in the body and other show nonspecific imaging features.

Conclusion

A variety of disease patterns involve the major salivary glands with few characteristic features on imaging. HRUS should be the first screening imaging tool followed by sialography, if required. CT is the mainstay of imaging in sialolithiasis while MRI is more optimal for neoplastic processes with associated invasion. CT and MRI are equally good in imaging of the cystic and inflammatory lesions especially abscesses.

References

1. La'Porte SJ, Juttla JK, Lingam RK. Imaging the floor of the mouth and the sublingual space. Radio Graphics 2011;31:1215-30.
2. Yousem DM, Kraut MA, Chalian AA. Major salivary gland imaging. Radiology 2000;216:19-29.
3. Liyanage SH, Spencer SP, Hogarth KM, Makdissi J. Imaging of salivary glands. Imaging 2007;19:14-27.
4. Drage NA, Brown JE. Cone beam computed sialography of sialoliths. Dentomaxillofacial Radiology 2009;38:301-5.
5. Hugill J, Sala E, Hollingsworth KG, Lomas DJ. MR sialography: The effect of a sialogogue and ductal occlusion in volunteers. Br J Radiol 2008;967:583-6.
6. Kalinowski M, Heverhagen JT, Rehberg E, Klose KJ, Wagner HJ. Comparative Study of MR Sialography and Digital Subtraction Sialography for Benign Salivary Gland Disorders. AJNR Am J Neuroradiol 2002; 23:1485-92.
7. Cho HW, Kim J, Choi J, Choi HS, Kim ES, Kim SH, *et al*. Sonographically Guided Fine-Needle Aspiration Biopsy of Major Salivary Gland Masses: A Review of 245 Cases. AJR Am J Roentgenol 2011;196:1160-63.
8. El-Khateeb SM, Abou-Khalaf AE, Farid MM, Nassef MA. A prospective study of three diagnostic sonographic methods in differentiation between benign and malignant salivary gland tumours. Dentomaxillofacial Radiol 2011;40:476-85.
9. Bialek EJ, Jakubowski W, Zajkowski P, Szopinski KT, Osmolski A. US of the Major Salivary Glands: Anatomy and Spatial Relationships, Pathologic Conditions, and Pitfalls. Radiographics 2006;26:745-63.
10. Yabuuchi H, Fukuya T, Tajima T, Hachitanda Y, Tomita K, Koga M. Salivary Gland Tumors: Diagnostic Value of Gadolinium-enhanced Dynamic MR Imaging with Histopathologic Correlation. Radiology 2003;226:345-54.
11. Yerli H, Aydin E, Habera N, Harman A, Kaskati T, Alibek S. Diagnosing common parotid tumours with magnetic resonance imaging including diffusion-weighted imaging versus fine-needle aspiration cytology: A comparative study. Dentomaxillofac Radiol 2010;39:349-55.
12. King AD, Yeung DK, Ahuja AT, Tse GM, Yuen HY, Wong KT, *et al*. Salivary gland tumors at *in vivo* proton MR spectroscopy. Radiology 2005;237:563-9.
13. Shah VN, Branstetter BF 4th. Oncocytoma of the parotid gland: A potential false-positive finding on 18F-FDG PET. AJR Am J Roentgeol 2007;189:W212-4.
14. Marchal F, Dulguerov P. Sialolithiasis management: The state of the art. Arch Otolaryngol Head Neck Surg 2003;129:951-6.
15. Christea A, Waldherrc C, Hallettd R, Zbaernb P, Thoenya H. MR imaging of parotid tumors: Typical lesion characteristics in MR imaging improve discrimination between benign and malignant disease. AJNR Am J Neuroradiol 2011;32:1202-7.
16. Patel ND, van Zante A, Eisele DW, Harnsberger HR, Glastonbury CM. Oncocytoma: The Vanishing Parotid Mass. AJNR Am J Neuroradiol 2011;32:1703-6.
17. Takagi Y, Sumi M, Sumi T, Ichikawa Y, Nakamura T. MR Microscopy of the parotid glands in patients with Sjögren's syndrome: Quantitative MR diagnostic criteria. AJNR Am J Neuroradiol 2005;26:1207-14.
18. Gododia A, Bhalla AS, Sharma R, Thakar A, Parshad R. Bilateral parotid swelling: A radiological review. Dentomaxillofac Radiol 2011;40:403-14.
19. Sato K, Gotoh C, Uchida H, Kawashima H, Yoshida M, Kitano Y, *et al*. Sialolipoma of the submandibular gland in a child. J Pediatr Surg 2011;46:408-10.

Cite this article as: Rastogi R, Bhargava S, Mallarajapatna GJ, Singh SK. Pictorial essay: Salivary gland imaging. Indian J Radiol Imaging 2012;22:325-33.
Source of Support: Nil, **Conflict of Interest:** No.